NOTES AND CORRESPONDENCE

The Spatial Structure of RASS Echoes

PETER T. MAY

Bureau of Meteorology Research Centre, Melbourne, Victoria, Australia

TATSUHIRO ADACHI, TOSHITAKA TSUDA

Radio Atmospheric Science Center, Kyoto University, Uji, Kyoto, Japan

RICHARD J. LATAITIS

Environmental Technology Laboratory, NOAA/ERL, Boulder, Colorado

22 November 1995 and 1 June 1996

ABSTRACT

An experiment to observe the spatial distribution of radio acoustic sounding system (RASS) echo intensity and Doppler shift using the MU radar is described. Various transmitting configurations are used to confirm that the RASS signal is focused onto a diffraction limited spot approximately the size of the transmitting antenna, except when a very small transmitting array is used where turbulence acting on the acoustic wave smears the spot. The signal fades away from the central spot with values about 6–10 dB lower in intensity next to the main spot. Significant gradients of Doppler shift across the radar antenna are seen in the lower height ranges. This may result in errors as large as a degree in the RASS virtual temperature estimates when large radar antennas and a single acoustic source are used.

1. Introduction

When RASS (radio acoustic sounding system) was first performed using a new generation of sensitive Doppler radars known as wind profilers, a major surprise was that the height coverage of the measurements was much greater than expected (May et al. 1988). Earlier work, building on the first practical RASS systems in the early 1970s (e.g., Marshall et al. 1972) suffered from very limited height coverage because of significant acoustic attenuation and the effect of wind displacing the acoustic wave fronts. The curvature of the acoustic waves provides a focusing effect, but wind displaces the acoustic waves shifting the "spot" away from the radar. Interest in the technique was rekindled when temperatures were measured to an altitude of over 20 km using the sensitive MU radar and steering the radar beam to correct for the wind displacement (Matuura et al. 1986). Subsequent studies using conventional wind profiler radars using vertically pointed beams showed that RASS applied to the new generation clear-air radars gave very useful height coverage, up to 5–10 km for 50-MHz wind profilers (May et al. 1988). Ray tracing calculations, similar to those of Masuda (1988), showed that useful measurements were obtained to heights about twice that of where the focused spot was displaced away from the radar antenna. A possible explanation for this was described in the theoretical work of Clifford et al. (1978), although the numerical results presented in that paper are in error and revised curves from Lataitis and Clifford (1996) will be shown here. Clifford et al. (1978) and others examined the spatial distribution of the RASS echo intensity and the effect of turbulent distortion of these waves. Calculations of the distribution of RASS signals affected by atmospheric turbulence showed a broadening of the diffraction limited spot and the raising of a background scattering level. The displacement of the sound waves by the wind moves the focus away from the radar antenna. May et al. (1988) hypothesized that they were primarily observing the raised background rather than the spot. However, the spatial distribution of echo intensity is not easy to measure and the theory is only now being tested (Bauer and Peters 1993).

This note presents observations of the spatial distribution of RASS echoes covering both the intensity distribution and its displacement with range as well as the

Corresponding author address: Dr. Peter T. May, Bureau of Meteorology Research Centre, GPO Box 1289K, Melbourne, Victoria 3001, Australia.
E-mail: p.may@bom.gov.au

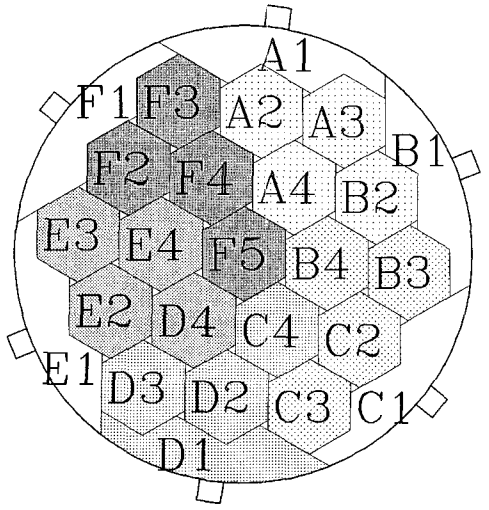

FIG. 1. Layout of the MU radar. The 25 groups of 19-antenna subarrays are shown. The alphanumeric labels indicate the various subarrays. Groups of four-antenna subarrays that are sampled together on reception have similar shading. The transmitter groupings used were 3 subarrays, F5C4D4; 7 subarrays, A4B4C4D4E4F4F5; 12 subarrays, A4B4C2C3D2D3E2E4F4F5C4D4; and 25 subarrays, whole antenna array.

way in which the Doppler shift varies across the region of detectable signals. These observations were taken with the MU radar (34.85°N, 136.10°E), near Kyoto. This radar is one of the world's most flexible clear-air Doppler radars. The antenna array is broken into 25 subarrays, and it is possible to transmit on any combination of antennas and receive the signals on each of the subarrays separately (Fig. 1). These observations have important implications for the height coverage and accuracy of RASS temperature measurements. The spatial gradient of RASS velocity may be a significant source of error at low height ranges in addition to the various geometric and turbulence induced errors (e.g., Angevine and Ecklund 1994; Peters and Angevine 1996), and the inexact correspondence between the speed of sound and virtual temperature (Kaimal and Gaynor 1991).

2. MU radar

The MU radar is a very flexible 46.5-MHz mesosphere–stratosphere–troposphere (MST) radar or wind profiler with a circular antenna array of 103-m diameter (see Fukao et al. 1985 for details). The important parameter for this study was that the array is broken up into 25 subarrays, each made up of 19 yagi antennas. Nineteen of these subarrays form a regular array of hexagons with the remaining six distributed about the periphery of the radar (Fig. 1). It is possible to transmit on any combination of subarrays and receive on the subarrays separately.

The radar beams can be steered in any direction within 30° of the zenith. This allows the beam to be steered to ensure that the radar beam is normal to the acoustic wave front so that the expected "focused" RASS echo falls on the MU antenna array (Matuura et al. 1986). For these experiments, a vertically pointing beam was used, similar to most wind profiler/RASS applications.

Since each antenna has its own transmitter unit, the total transmitted radar power, and hence sensitivity, is proportional to the number of units used. The scattered signal was sampled on the 19 central subarrays separately. Since reception is on single units, the sensitivity of the system compared to when the entire array is used for reception is diminished.

However, there were only four receiver channels, so that only four groups could be sampled at a time. Each antenna group was sampled for a period of 18.2 s, before another set of four were selected. Thus, the cycle to sample the entire receiving array was completed in 130 s, after which a new transmitter configuration was chosen. The Doppler spectra of the backscattered signal were stored on magnetic tape for postanalysis.

The Nyquist velocity for the spectra of the backscattered signal was 22.6 m s^{-1}, with the receiver center frequency offset to allow detection of the RASS echo peak. The velocity resolution is 0.18 m s^{-1} (i.e., the time series were 256 points long). A height resolution of 300 m was used for these experiments with the lowest reliable height being 1.5 km above ground level.

The two parameters of interest in the spectra are the backscattered power and mean Doppler shift. The power and mean Doppler shift are estimated by directly calculating the zeroth- and first-order moments.

The MU radar has been operating for over 10 years and some of the antenna subarrays had decreased sensitivity. This effect has been corrected for in the analysis using clear-air data before and after the RASS mapping. The amplitude of clear-air scatter is expected

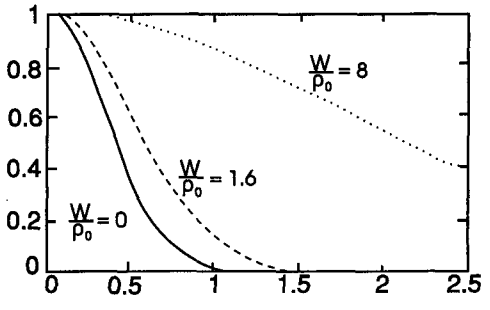

FIG. 2. Theoretical calculations for the intensity of the backscattered signal for a Gaussian illumination function as a function of a normalized distance from the center of the spot r/D, where D is the antenna diameter. The curves correspond to no turbulence, moderate, and severe turbulence (W/ρ_0 = 0, 1.6 and 8) (adapted from Lataitis and Clifford 1996).

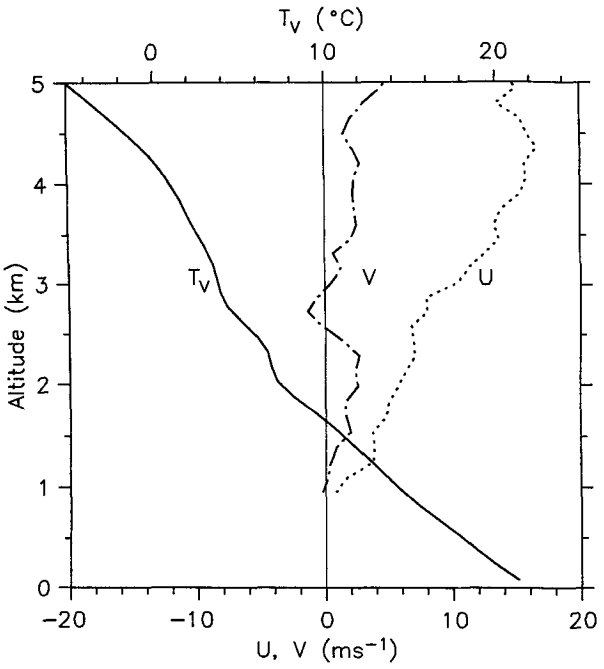

FIG. 3. Profiles of the zonal and meridional wind component derived from MU radar observations between 1635 and 1745 LT 12 September 1993 (covering the RASS period) and a profiler of virtual temperature measured by a radiosonde launched at 1440 LT. The altitude in this and all subsequent figures is given above ground level.

to be uniform across the radar array. Therefore, the clear-air echo strength has been used to calibrate the subarray sensitivity for the RASS measurements. Measurements were performed with the same transmitter combinations as for the RASS to allow accurate corrections of the receiver array sensitivity. However, for two of the subarrays (C2 and C4), no correction is possible because the sensitivity was reduced so far that no RASS echoes were detectable.

To investigate the effect of antenna size on the scattered field, successive experiments were done using quasi-circular groups consisting of 3, 7, 12, and 25 subarrays for transmission. A transmitter configuration was used for a period of about 130 s. The period was kept as short as possible to minimize the effect of temporal changes.

A five-beam wind sounding, which is the conventional MU radar observation, was then performed to check for changes in wind speed and direction. This was then followed by the next RASS observation with a new transmitter configuration. There was no significant change of wind velocity over the observation period.

These experiments were first performed in September 1992 with a commercial amplifier–loudspeaker system (Tsuda et al. 1994) using a triangular linear frequency sweep between 90 and 110 Hz and back to 90 (e.g., May et al. 1990). The experiment was repeated on 11 September, 1993 using a high power pneumatic acoustic generator (Tsuda et al. 1989). The pneumatic system forces the use of acoustic pulses. However, the frequency was modulated within the pulse with the instantaneous frequency being swept up from 97.6 to 110 Hz. With such a chirped pulse, it appears that the dominant returns are only from that part of the spectrum that is Bragg matched, so that there is only a single Bragg peak rather than the possible double-peaked spectrum where simple pulses are employed (May et al. 1990).

The returned echo power was greater in the 1993 experiment because of the increased acoustic power. Therefore, the discussion on echo power will concentrate on the 1993 results. The data in 1992 showed similar trends but were noisier. The horizontal wind was also larger in 1992 causing greater displacement of the echo pattern. The horizontal wind also has an impact on the distribution of the RASS Doppler shift across the antenna. This is more pronounced in the earlier data because of the greater wind speed. Therefore, discussion on the distribution of the RASS Doppler shift will focus on the earlier experiment.

3. Theoretical background

The RASS technique relies on the radar backscatter from fluctuations in air density associated with a sound wave. The Doppler shift of the scattered signal is determined by the speed of sound, which in turn is related to the virtual temperature; thus this technique allows high-resolution (in time and height) remote sensing of temperature profiles. Resonant backscatter occurs when the acoustic wavelength is half the radar wavelength (Bragg condition). Furthermore, there is a focusing effect produced by the curvature of the acoustic waves.

There was theoretical work performed by Clifford et al. (1978) and others in the mid-1970s studying the spatial distribution of RASS echo power. Clifford et al. calculated the spatial distribution for the case of a uniform amplitude antenna polar diagram with a fixed beamwidth and with the effect of turbulence on the acoustic waves included. Although the basic theory was correct, there was, however, an error in the nu-

TABLE 1. Turbulence parameters and transmitter beam dimensions for a height of 3.5 km and a boundary layer depth of 2 km with $C_n^2 = 5 \times 10^{-8}$ m$^{2/3}$ in the boundary layer; $\bar{C}_n^2 = 1.1 \times 10^{-8}$ m$^{2/3}$. The acoustic coherence length ρ_0 is 281 m.

Number of subarrays	Width of beam (m)	$\frac{W}{\rho_0}$	Antenna diameter (m)	Spot diameter D_s (m)
3	797	2.83	28	49
7	445	1.58	51	64
12	343	1.22	66	77
25	219	0.78	103	111

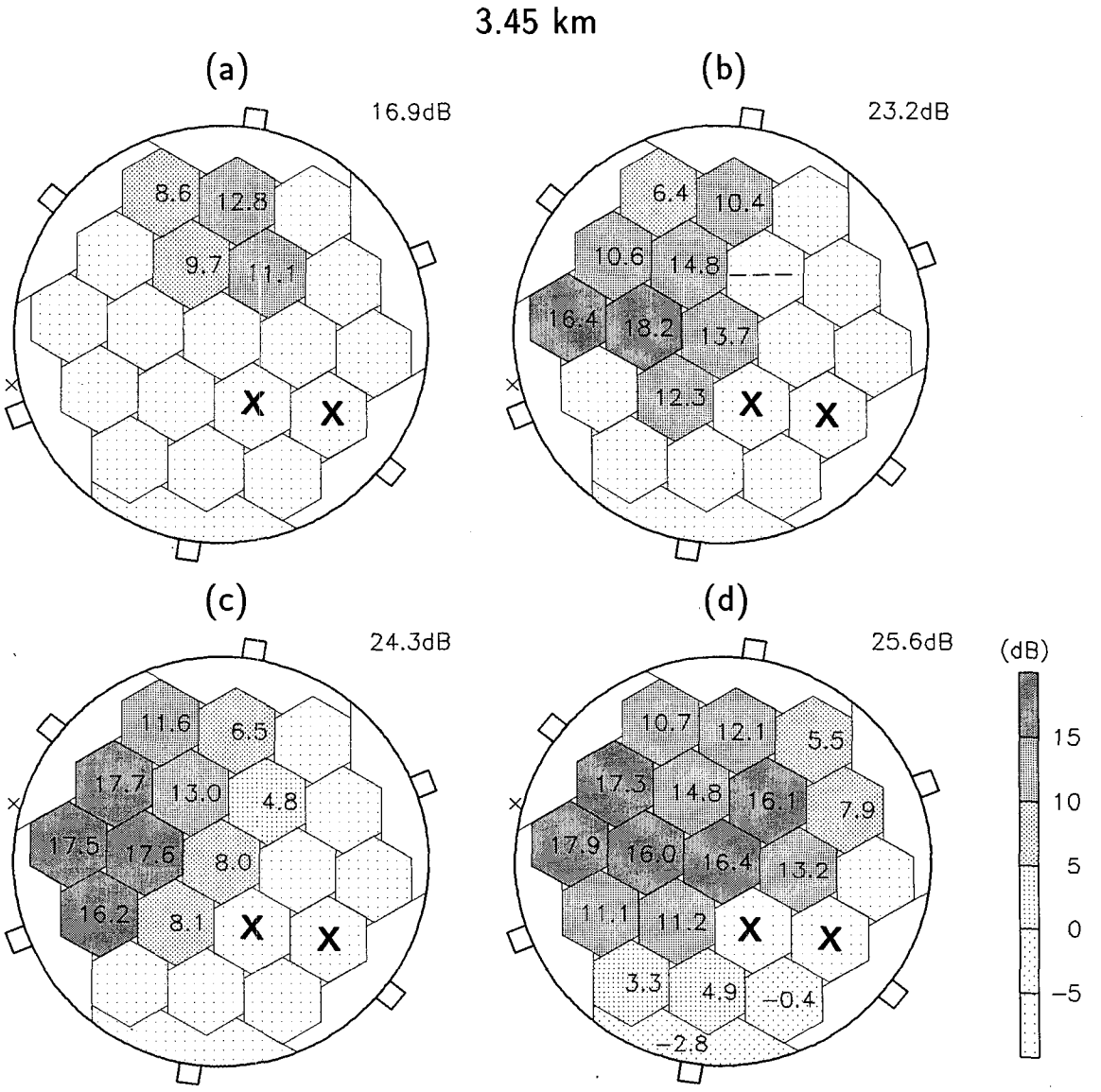

FIG. 4. Distribution of echo power (dB) for transmission on groups of (a) 3, (b) 7, (c) 12, and (d) 25 groups of antennas. The height sampled is 3.45 km. The subarrays marked with a cross had insufficient sensitivity to observe RASS echoes. The location of the acoustic source is shown by the small cross on the periphery of the antenna on the western side. The total received power is given in the top right of each figure.

merical calculations (Lataitis and Clifford 1996) and this integral equation for the spatial distribution of echo paper has been recalculated (Fig. 2). If turbulence and the effect of stratification on the speed of sound, and hence acoustic wavefront shape, are ignored, both the incident electric field and acoustic waves can be represented as spherical wave fronts. These results showed that if the effect of turbulence is negligible and the radar beamwidth is much narrower than the acoustic beamwidth (this is often the case with wind profiler/RASS, although boundary layer profiler/RASS systems may have comparable acoustic and radar beamwidths), the scattered field distribution at the ground should be very similar to the radar illumination field pattern. In the limit of an isotropic acoustic source, then the spot has an identical shape to the radar antenna illumination. However, Lataitis and Clifford (1996) also show that for a uniform antenna illumination (as we have here) and weak turbulence the edges of the scattered field distribution are eroded and a tail of echo intensity extends beyond the illumination diameter giving a region of most intense power smaller than the antenna size (their Fig. 2b). The effect of intense levels of turbulence is to perturb the acoustic wavefronts and

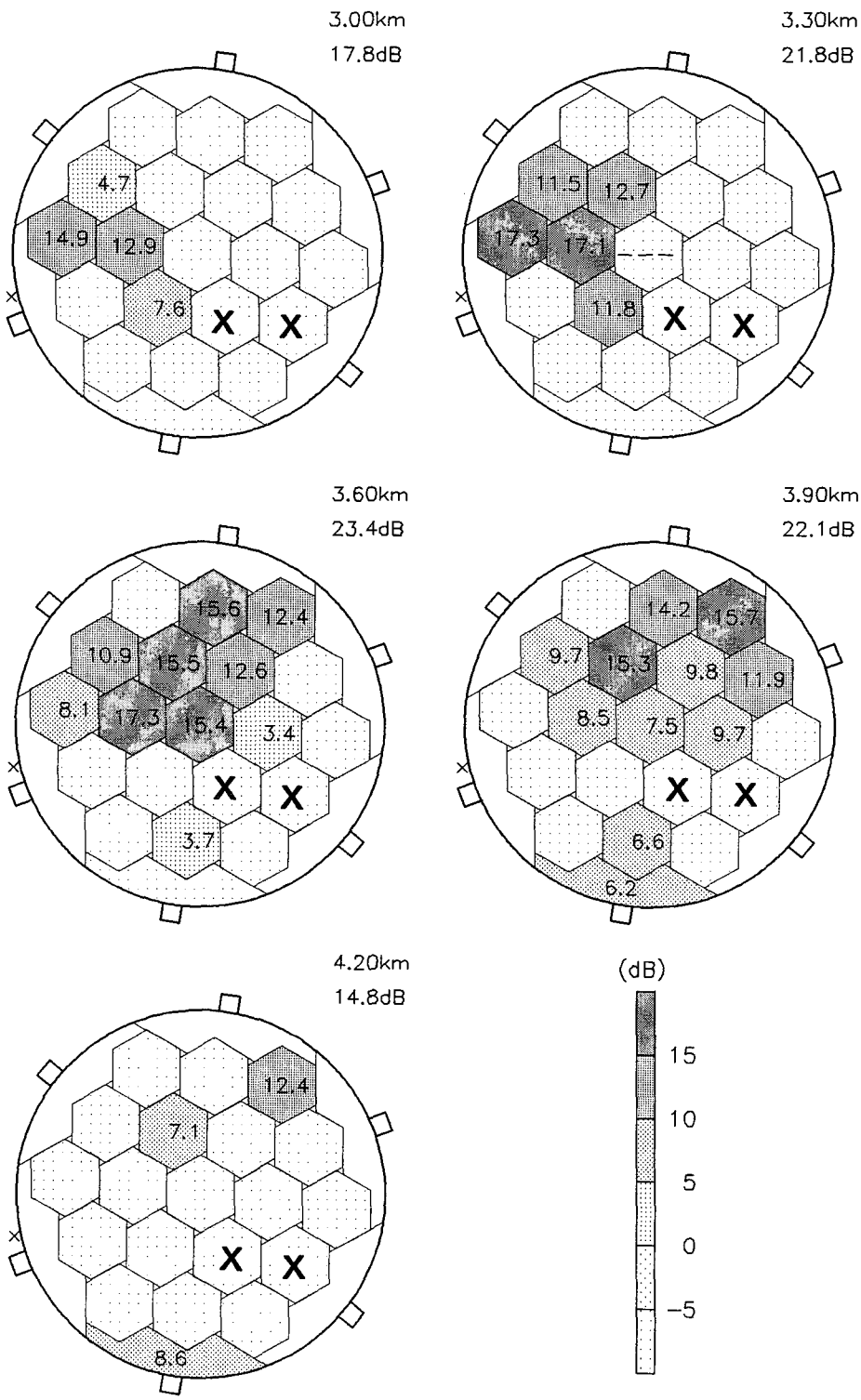

FIG. 5. As in Fig. 3 but showing a height sequence for transmission on seven subarrays.

smear the spot (Lataitis 1992; Bauer and Peters 1993; Lataitis and Clifford 1996). Recent measurements with a 24-cm-wavelength radar support the turbulence induced increase in echo power away from the main spot (Bauer and Peters 1993).

This raises the question of how much broadening is expected. Following Lataitis (1992), it is possible to examine this for the transmitter configurations. The mean structure parameter $\bar{C}_n^2$ averaged to a height R is

$$\bar{C}_n^2 = \frac{8}{3} R^{-8/3} \int_0^R C_n^2 z^{5/3} dz. \quad (1)$$

If we assume that $\bar{C}_n^2$ is dominated by high values in the boundary layer and that the turbulence level is constant in this layer, then at a height R and a boundary layer depth R_b:

$$\bar{C}_n^2 = R^{-8/3} C_n^2 R_b^{8/3}, \quad (2)$$

where C_n^2 is the value in the value of the structure parameter in the boundary layer. A typical value of C_n^2 for acoustic waves in the boundary layer is about 5×10^{-8} m$^{-2/3}$. Figure 3 shows a profile of the virtual temperature measured by a radiosonde ascent. Note the change of slope from values close to the dry adiabat near a height of 2 km above the ground indicating the top of the boundary layer. This results in a value of $\bar{C}_n^2$ of 5×10^{-8} m$^{-2/3}$ at the top of the boundary layer and 1.1×10^{-8} m$^{-2/3}$ at 3.5 km.

The coherence length ρ_0 of the acoustic wave is given by

$$\rho_0 = (0.546 k_a^2 R \bar{C}_n^2)^{-3/5}, \quad (3)$$

where k_a is the acoustic wavenumber ($2\pi/3.22$ m^{-1}). This can be compared to the horizontal extent of the radar beam ($W \sim \lambda R/D$ where D is the transmitting antenna diameter) and weak turbulence is in the regime where $W < \rho_0$. Values for the various transmitter configurations and are given in Table 1 (the value of W/ρ_0 is almost constant above R_b). Note that the small array is expected to be strongly affected by turbulence, while the middle two values are in a moderate regime. The use of the whole array puts the data in a weak turbulence regime. Different choices of C_n^2 obviously change these thresholds slightly.

Since the pattern on the ground represents a convolution of the turbulence effect with the antenna illumination, it is possible to estimate the spot diameter from the value of ρ_0. The angle defined by a diameter of $2\rho_0$ at a distance R can be related to a pseudoillumination width $\lambda R/2\rho_0$ (assuming $R \gg 2\rho_0$), where λ is the radar wavelength and the effective spot diameter D_s becomes

$$D_s \approx \left[D^2 + \left(\frac{\lambda R}{2\rho_0} \right)^2 \right]^{0.5} \approx \left[\left(\frac{\lambda R}{W} \right)^2 + \left(\frac{\lambda R}{2\rho_0} \right)^2 \right]^{0.5}. \quad (4)$$

These relations illustrate the relative importance of the horizontal extent of the radar beam and the correlation distance of the acoustic wave. Values of D and D_s are given in Table 1. This again illustrates that turbulence will be most apparent with the small antenna aperture because W becomes large. Since the receiving arrays have a finite size, the actual measured pattern is a convolution of the backscattered pattern with the receiving antenna response, but in practice this is not important since the receiving antennas are much smaller than D_s.

Profiler/RASS systems operating in the UHF band (400, 900 MHz and higher) will generally be in a high turbulence regime at ranges greater than a few hundred meters when there is a reasonably deep boundary layer.

4. Experiment and results

a. Distribution of echo power

As noted, the total transmitted power is proportional to the size of the transmitting array in the MU radar. The measured signal-to-noise ratio (SNR) has been normalized to remove the effect of this variable transmitter power so that the received power levels in various configurations can be compared. There is not expected to be much change in the echo distribution during the data acquisition, as each "map" is produced with just over 2 min of data. However, maps cannot be averaged as the position of the centroid of the pattern changes significantly during the time between successive maps with the same transmitter configuration (~35 min).

Figure 4 shows plots of the normalized SNR at a height of 3.45 km for each of the transmitter configurations. These figures show several significant features. In particular, there is a principal echo region with values between 15 and 18 dB about half of the size of the transmitter array. The signal power surrounding the peak fades away with values about 5 dB lower next to the peak, extending out to about the area of the transmitting antenna size or slightly larger and no detectable signals farther away from the main lobe. The amplitude of this enhanced region is similar for all the cases (i.e., the received power is fairly independent of the transmitting antenna gain), except for the smallest transmitter array case, which is lower. This is expected once the transmitter power has been calibrated out. All the experiments are employing wide beam receiving antenna arrays. At first, it may seem that stronger returns would be obtained from the use of higher gain (narrow beamwidth) transmitting antennas, but in such a bistatic configuration with wide receiving antennas the increased gain of transmission is offset by the associated decrease in the radar pulse volume. Another way to look at this is that the receiving and transmitting pulse volumes are different, and the receiving pulse volume is not filled. In normal monostatic operation, the receiving antenna gain becomes important, and the

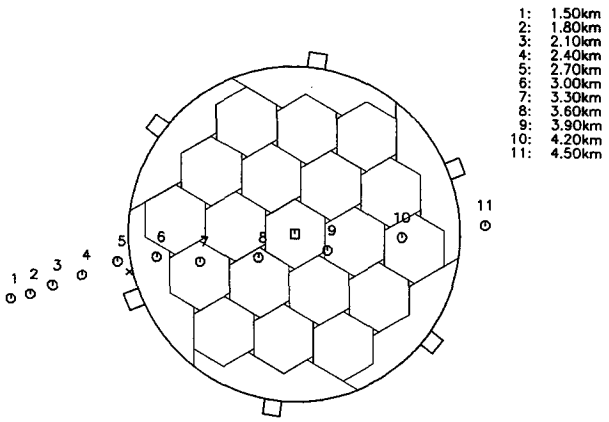

FIG. 6. Spot positions vs height deduced by a ray tracing algorithm. The wind was assumed to vary linearly from zero at the surface to the lowest wind measurement with the MU radar at 1.7 km. The points are at 300-m intervals beginning at 1.5 km.

returned signals will be related to the antenna gain. Indeed, the total returned power, integrated over the radar antenna, does increase for larger transmitter array sizes as the spot diameter increases by approximately the square root of the number of transmitting subarrays. The exception is the case of three transmitting antennas in which both the peak and the total power are less than expected compared to the use of larger arrays. This may be a result of the greater influence of turbulence when small arrays (with large beamwidths) are used. Turbulence causes a decrease in the returned power (Clifford and Wang 1977; Clifford et al. 1978; Bhatnagar and Peterson 1979). The "lumpy" nature of the reflectivity distributions probably reflects the effect of turbulence on the acoustic waves and temporal changes over the 130-s data acquisition period. The size of the enhanced region is clearly related to the size of the transmitting array, as expected from theoretical considerations.

The winds were consistently from the west, but with considerable shear of wind speed with height during the 1993 experiment (Fig. 3). The advection of the sound waves by the wind is clearly illustrated in Fig. 5, which shows the echo intensity distribution as a function of height. The enhanced region moves across the array with height at a speed close to twice the horizontal wind speed as predicted by geometric arguments. Ray tracing (e.g., Masuda 1988) has been performed to estimate the displacement of the center of the RASS "spot" across the array. The wind speed was assumed to increase linearly from the surface to the lowest MU radar observed wind. The results of the ray tracing are shown in Fig. 6. The observed displacements are consistent with the ray tracing with some offset to the north, probably associated with the winds in the lowest few hundred meters. There is also some evidence for increased relative power away from the main lobe with height. This effect is expected if the acoustic wave is increasingly distorted by atmospheric turbulence (Lataitis 1992). However, if the turbulent distortion is dominated by the expected higher turbulent intensity in the boundary layer, and the observations are above this layer, then there may be little further smearing with increased height.

b. Doppler shift distribution

Figure 7 shows the RASS sound speed detected for each antenna element across the antenna array at two heights during a period in the earlier 1992 experiment: one being the lowest height for detectable RASS measurements, and the other near the maximum height with good SNR. A consistent pattern is seen at the lower height with a value of the RASS Doppler shift increasing toward the southern part of the array. The actual variation across the array is considerable: approxi-

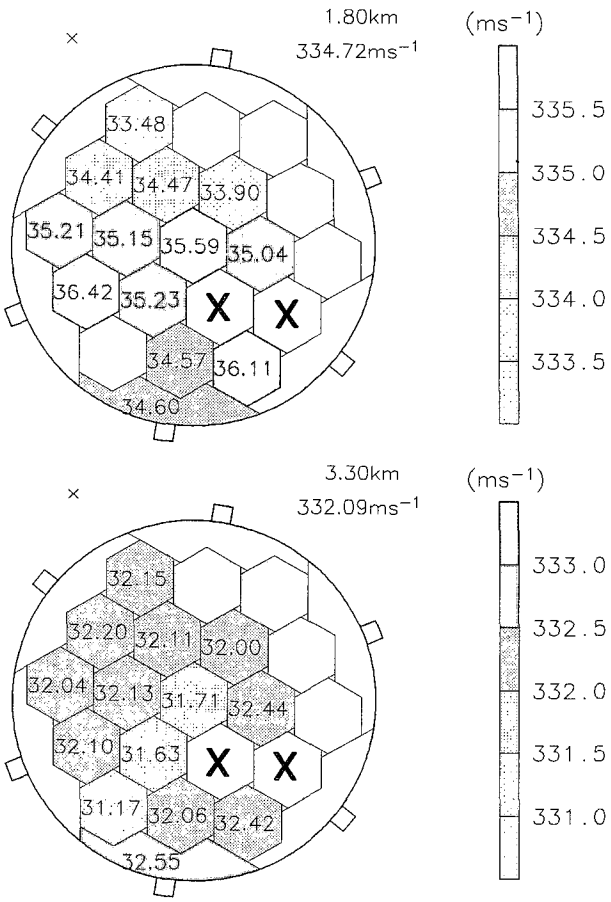

FIG. 7. A distribution of the RASS Doppler shift across the receiving array for 1.8 and 3.3 km during the 1992 experiment. Transmission was using the full 25 subarrays. The numbers represent the speed of sound (-300 m s^{-1}). The acoustic source is located at the small cross on the northern side of the array. The reflectivity weighted mean Doppler shift is shown on the top right.

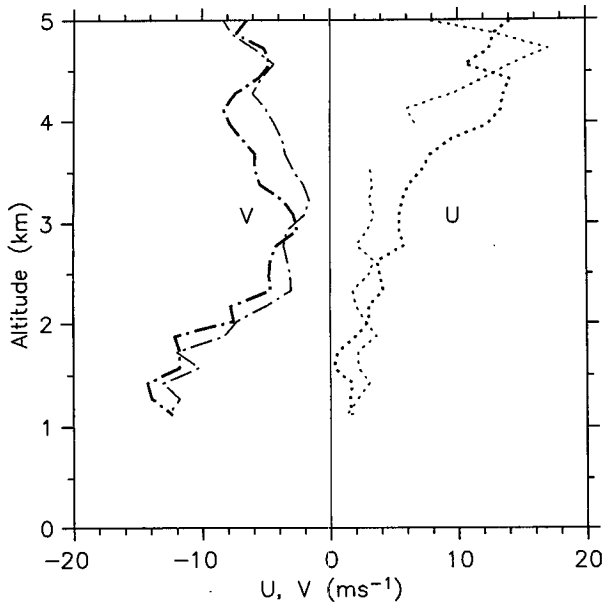

FIG. 8. Profiles of the zonal (u) and meridional (v) wind velocity profiles for 0147–0149 LT (thick) and 0225–0227 LT (thin) on 12 September 1992. These profiles are before and after the RASS observations discussed in Fig. 7.

mately 1.2 ± 0.9 m s^{-1} in the direction of the wind, which corresponds to about a 2°C range of measured temperatures. However, the RASS velocities are much more uniform at the upper height with a negligible gradient across the array (0.2 ± 0.6 m s^{-1}). For reference, profiles of the wind components are shown in Fig. 8. Note the wind speed is in excess of 15 m s^{-1} at the lower heights suggesting a pronounced low-level jet. The smaller effect at the upper height could be related to a smaller wind speed, but no significant variations of velocity across the antenna were observed at upper heights in the 1993 experiment, even though the wind speed was comparable to the low-level winds in 1992.

The large gradient observed across the radar at the lower heights is disturbing as it indicates that there is the potential for considerable error in temperature measurements at the lower heights if the RASS spot is displaced off the radar centroid. In general, the use of the entire antenna array will decrease this error. However, if the radar is only sampling the edge of the "spot" such as when offset acoustic sources are used, then errors as large as a degree are possible at the lower heights with large antenna arrays.

To attempt to explain these observations, it must first be remembered that we are essentially dealing with a bistatic radar system. The observed gradient is consistent with the notion that the centroid of the contributions to the received signal is displaced to virtually above the receiving array allowing a significant "leakage" of the horizontal wind. As the range increases, the angle between two lines, one drawn from the transmitter array to the point directly above the receiving array and one from that point to the receiving array, decreases. However, there are serious difficulties with this explanation.

First, consider an acoustic wavefront centered over the (narrowbeam) transmitter array, moving outward at a speed c_a, and advected horizontally at a speed u (Fig. 9). If each point along the wave front can be considered as an isotropic scatterer, the mean velocity may be estimated by considering the phase difference of each point between the initial time and some time δt, and just estimating a mean weighted by the product of transmitting and receiving antenna illuminations. This product is biased over the transmitting antenna (since its polar diagram is much narrower than the receiving array polar diagram) and actually produces a (small) bias in the opposite sense to the observed gradient. Furthermore, if some correction is made for the fact that the bisector of the angle between two lines, one drawn from the transmitter antenna to a scattering point and the second from the point to the receiving antenna, is not perpendicular to the wave front when the antennas are displaced, the departure from perpendicularity decreases toward the opposite side of the wave front to the receiving antenna's displacement, again producing biases of the opposite sign to that which is observed.

Thus, it appears a more complete theoretical calculation is required. Peters and Kirtzel (1994) considered the effect of displacements of the acoustic wave from overhead and found significant biases could be intro-

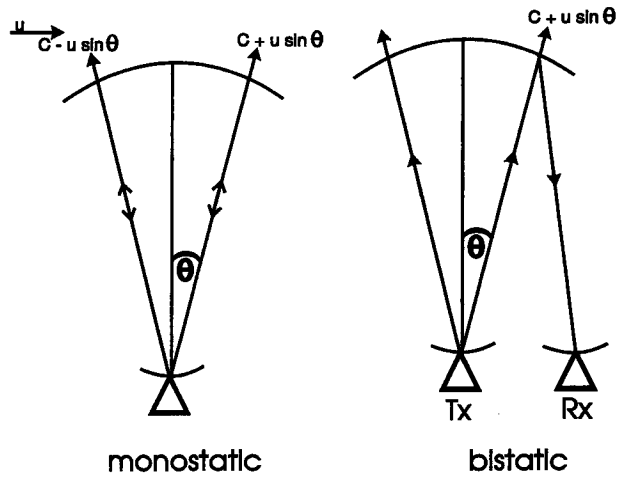

FIG. 9. Schematic illustrating the leakage of the horizontal wind into the RASS Doppler shift across an antenna array. When the acoustic wave is directly over the array, the contributions to the RASS echo are from an area symmetrically about the zenith for the case of a monostatic radar, so only the speed of sound c contributes to the Doppler shift and the wind merely broadens the spectral width of the received signal. But when the receiving antenna is displaced horizontally, the contributions to the RASS echo may not be symmetric allowing the horizontal wind to leak into the measured Doppler shift.

duced, particularly at lower heights. The effect we are observing here may be related as the use of different receiving subarrays changes the relative positions of the acoustic wave fronts with respect to the radar system.

Profilers operating at higher frequencies have correspondingly small antennas and physical separation between the antenna arrays and sound sources. Therefore, this geometric effect will only be important at quite low heights. For example, where a 100-m antenna sees large effects up to 2.5 km, a 2-m antenna, typical of UHF wind profilers will have a similar effect only up to 50 m. In practice, the relative displacements (measured in wavelengths) of the radar antenna and acoustic sources at the ground are slightly higher for UHF profilers so the effects will be seen somewhat higher than 50 m.

An additional error may also arise if there is a vertical velocity correction. Since the clear-air peak is a volume average, the line of sight clear-air Doppler peak may be from a different effective angle than that of the RASS echo, which introduces a further source of error.

Similar results were seen in the 1993 experiment, but the wind was relatively weak, particularly at the lower heights (Fig. 4). Therefore, while there was a significant trend across the antenna array, the random errors in measuring the Doppler shift produce a noisier pattern (not shown).

It is expected that these effects will be decreased if multiple acoustic sources were used since the likelihood of the maximum reflectivity center being displaced a large distance from the zenith is reduced, particularly at the lower ranges where this effect will be largest.

5. Discussion

Experiments to measure the distribution of any kind of radar echo power across the ground are difficult. This is particularly true for RASS where a region of enhanced power is systematically displaced by the wind, and the displacement is an integral effect of the wind profile. An experiment to test the theory of the RASS echo distribution has been performed using a unique radar facility.

The observations confirm many of our ideas concerning the distribution of RASS echoes. In particular, the existence of a diffraction limited spot has been demonstrated. The spot consists of an intense echo region about half of the transmitting antenna size surrounded by an area of weaker intensity. This is consistent with theoretical calculations for the expected distribution characteristics in conditions of weak to moderate turbulence (Lataitis and Clifford 1996). This is most evident when using the small transmitting array. A region around the peak with a signal level 5–10 dB below that of the maximum intensity is seen, even at low altitudes. It also appears that the turbulent distortion of the acoustic waves has decreased the amplitude of the backscattered power when using the small transmitter array. These results are broadly consistent with the results of Bauer and Peters (1993) and Lataitis and Clifford (1996).

Significant gradients of apparent sound speed were seen across the antenna array. This is consistent with a geometric leakage of the horizontal wind into the sound speed measurements and combined with the spatial gradients of RASS reflectivity may be a significant source of error. These observations also provide a test for theoretical studies, which until now have concentrated primarily on the signal intensity distribution.

It is reasonable to expect that similar experiments with multiple acoustic sources, as are widely used (May et al. 1990), will produce multiple spots and mitigate the effect of displacement of the spots by wind. The use of multiple acoustic sources may also reduce errors in temperature estimates due to the spatial gradient of the Doppler shift. For the case of profilers with large antennas looking at low altitudes, the errors introduced by the spatial gradients of Doppler shift may be significant but are likely to be correspondingly small for UHF wind profilers.

Acknowledgments. PTM would like to thank the staff at RASC for the opportunity of visiting and performing the experiment described in this paper. Their kind hospitality is fondly appreciated. The authors also acknowledge the contributions of the reviewers, which have greatly improved the paper.

REFERENCES

Angevine, W. M., and W. L. Ecklund, 1994: Errors in radio acoustic sounding of temperature. *J. Atmos. Oceanic Technol.*, **11,** 837–842.

Bauer, M., and G. Peters, 1993: On the altitude coverage of temperature profiling by RASS. Preprints, *26th Int. Conf. on Radar Meteorology,* Norman, OK, Amer. Meteor. Soc., 487–489.

Bhatnagar, N., and A. M. Peterson, 1979: Interaction of electromagnetic and acoustic waves in a stochastic atmosphere. *IEEE Trans. Antennas Propag.,* **AP-27,** 385–393.

Clifford, S. F., and T. I. Wang, 1977: The range limitation on radar-acoustic-sounding-systems (RASS) due to atmospheric refractive turbulence. *IEEE Trans. Antennas Propag.,* **AP-25,** 319–326.

——, T. Wang, and J. T. Priestly, 1978: Spot size of the radar return from a radar-acoustic sounding system (RASS) due to atmospheric refractive turbulence. *Radio Sci.,* **13,** 985–989.

Fukao, S., T. Sato, T. Tsuda, S. Kato, K. Wakasugi, and T. Makihara, 1985: The MU radar with an active phased array system 1: Antenna and power amplifiers. *Radio Sci.,* **20,** 1155–1168.

Kaimal, J. C., and J. E. Gaynor, 1991: Another look at sonic thermometry. *Bound.-Layer Meteor.,* **56,** 401–410.

Lataitis, R. J., 1992: Signal power for acoustic sounding of temperature: The effects of horizontal winds, turbulence and vertical temperature gradients. *Radio Sci.,* **27,** 369–385.

——, and S. F. Clifford, 1996: The effect of turbulence on the spot size of a RASS echo: A calculation revisited. *Radio Sci.,* in press.

Marshall, J. M., A. M. Peterson, and A. A. Barnes Jr., 1972: Combined radar-acoustic sounding system. *Appl. Opt.,* **11,** 108–112.

Masuda, Y., 1988: Influence of wind and temperature on the height limit of a radio acoustic sounding system. *Radio Sci.,* **23,** 647–654.

Matuura, N., Y. Masuda, H. Inuki, S. Kato, S. Fukao, T. Sato, and T. Tsuda, 1986: Radio acoustic measurement of temperature profile in the troposphere and stratosphere. *Nature,* **333,** 426–428.

May, P. T., R. G. Strauch, and K. P. Moran, 1988: The altitude coverage of temperature measurements using RASS with wind profiler radars. *Geophys. Res. Lett.,* **15,** 1381–1384.

——, ——, ——, and W. L. Ecklund, 1990: Temperature sounding by RASS with wind profiler radars: A preliminary study. *IEEE Trans. Geosci. Remote Sens.,* **28,** 19–28.

Peters, G., and H. J. Kirtzel, 1994: Measurements of momentum flux in the boundary layer by RASS. *J. Atmos. Oceanic Technol.,* **11,** 63–75.

——, and W. M. Angevine, 1996: On the correction of RASS temperature errors due to turbulence. *Beitr. Atmos. Phys.,* **69,** 81–96.

Tsuda, T., Y. Masuda, H. Inuki, K. Takahashi, T. Takami, T. Sato, S. Fukao, and S. Kato, 1989: High time resolution monitoring of the tropospheric temperature with a radio acoustic sounding system (RASS). *Pure Appl. Geophys.,* **130,** 497–507.

——, T. Adachi, and Y. Masuda, 1994: Observations of temperature fluctuations with the MU radar–RASS. *J. Atmos. Oceanic Technol.,* **11,** 50–62.